Carbohydrate Polymers 300 (2023) 120256

Contents lists available at ScienceDirect

Carbohydrate Polymers

journal homepage: www.elsevier.com/locate/carbpol

Pickering emulsions with chitosan and macroalgal polyphenols stabilized by layer-by-layer electrostatic deposition

Weihao Meng [a,b,1], Hongnan Sun [a,*,1], Taihua Mu [a,*], Marco Garcia-Vaquero [b,*]

[a] Laboratory of Food Chemistry and Nutrition Science, Institute of Food Science and Technology, Chinese Academy of Agricultural Sciences; Key Laboratory of Agro-Products Processing, Ministry of Agriculture and Rural Affairs, No.2 Yuan Ming Yuan West Road, Haidian District, P.O. Box 5109, Beijing 100193, PR China
[b] School of Agriculture and Food Science, University College Dublin, Belfield, Dublin 4, Ireland

ARTICLE INFO

Keywords:
Macroalgal polyphenols
Chitosan
Pickering emulsion
Emulsifying property
Structure characterization

ABSTRACT

Due to the hydrophilic nature of chitosan, its use as stabilizers in Pickering emulsions requires of hydrophobic modifications that can be achieved by layer-by-layer electrostatic deposition. This study aims to explore and optimize the effects of multiple parameters (chitosan-polyphenol ratio, chitosan concentrations, oil-phase ratios, pH and NaCl concentrations) on the stability of Pickering emulsions stabilized by chitosan and macroalgal polyphenols. The binding mode of chitosan and polyphenols in co-stabilized Pickering emulsions was characterized by Fourier transform infrared spectroscopy (FTIR), confocal scanning laser microscopy (CLSM), scanning electron microscopy (SEM), atomic force microscopy (AFM), and contact angle. The emulsions had the highest physical stability (95.67 %) and specific surface area (2.21 m^2/g) at: chitosan-polyphenol ratio 9.5:1 (w:w), chitosan concentration 0.5 % (*w/v*), oil-phase ratio 5 % (*v*/v), pH 6, and NaCl concentration 0 mM. FTIR, CLSM, SEM, and AFM evidenced that chitosan and polyphenols were bound by hydrogen bonds and electrostatic interactions at oil-water interfacial layers of emulsions that had a contact angle of 87.8°, indicating that polyphenols combined with chitosan had better ability to stabilize Pickering emulsions compared to chitosan alone. This study broadens the potential applications of naturally extracted macroalgal polyphenols for the development of Pickering emulsions in nutraceutical and functional food industries.

1. Introduction

Emulsions, which are complex mixtures of two partially/completely immiscible liquids (i.e., water and oil) have been used as delivery systems to encapsulate bioactive compounds with pharmaceutical, cosmeceutical and nutraceutical properties. Traditional surfactant-stabilized emulsions could be easily de-stabilized due to processes of creaming, coalescence, flocculation and Ostwald ripening, hindering their potential applications (McClements & Jafari, 2018). Thus, the development of Pickering emulsions stabilized by solid particles, more stable compared to emulsions generated by classic surfactants, has recently attracted the interest of the food industry (Zhu et al., 2021). Consumers' awareness and attitudes towards chemicals in food formulations and more particularly surfactants are perceived negatively (Jo et al., 2021).

Currently, Pickering emulsions are excellent alternative for encapsulating and delivering a variety of high-value compounds, such as β-carotene (Yi et al., 2021), curcumin (Zhu et al., 2021), astaxanthin (Ge et al., 2022), docosahexaenoic acid (DHA) (Liu et al., 2021), and resveratrol (Jo et al., 2021) due to their easy formulation, non-toxicity, and long-term stability.

Several inorganic and synthetic solid particles, such as silicon and titanium dioxides, are considered as excellent Pickering emulsion stabilizers. However, these inorganic particles are non-biodegradable and non-biocompatible, limiting their widespread use for applications in the food and pharmaceutical industries (Chevalier & Bolzinger, 2013). In recent years, food-derived compounds, such as polysaccharides, proteins, flavonoid crystals, food-grade waxes and fat crystals, have been successfully explored as stabilizers in Pickering emulsions (Xia et al., 2021).

Layer-by-layer (LBL) deposition is a common emulsion preparation method that improves emulsion's stability. This technique typically uses two stabilizers with opposite charges to deposit at the oil-water (O/W) interface of the emulsion to form stable droplets (Aoki et al., 2005). The

* Corresponding authors.
E-mail addresses: sunhongnan@caas.cn, honey0329@163.com (H. Sun), mutaihua@126.com (T. Mu), marco.garciavaquero@ucd.ie (M. Garcia-Vaquero).
[1] These authors contributed equally: Weihao Meng, Hongnan Sun.

https://doi.org/10.1016/j.carbpol.2022.120256
Received 22 August 2022; Received in revised form 2 October 2022; Accepted 20 October 2022
Available online 26 October 2022

selection of a suitable combination of stabilizers is crucial for an efficient generation of emulsions using this method. Chitosan is a cationic polysaccharide that offers multiple advantages as stabilizer, as it is relatively inexpensive, commercially available, biocompatible, and biodegradable, and widely used for biomedical, pharmaceutical and food applications (Shah, Dvořák, et al., 2021). Complexation of chitosan with other molecules makes it more surface-active, by modulating its wettability, leading to a higher stability of co-stabilized Pickering emulsions (Sharkawy et al., 2020). Amongst these molecules, the use of natural polyphenols could be promising. Polyphenols are usually negatively charged and have been used to form complexes with positively charged biopolymers to stabilize Pickering emulsions (Zembyla et al., 2019). Polyphenols were reported to act as cross-linking agents bonding chitosan in Pickering emulsions (Zhao et al., 2022), composite fibres (Zhu et al., 2019) and films (Sionkowska et al., 2015). In addition, polyphenols have been shown to improve the dispersion and oxidative stability of emulsion systems (Di Mattia et al., 2010). Polyphenols from macroalgae have recently received an increased interest from the scientific community due to their wide range of biological activities (Dong et al., 2019; Heffernan et al., 2015; W. Meng et al., 2021; Meng, Mu, et al., 2022). Previous research optimized the extraction of polyphenols from the macroalgal *A. nodosum*, achieving purities of 73.85 % (Meng et al., not published yet). Macroalgal polyphenols are a class of poorly water-soluble polyphenols (Bai et al., 2020), and previous reports identified the use of other water-insoluble polyphenols as good stabilizers in Pickering emulsions (Zembyla et al., 2019). However, there are currently no studies on the application of polyphenols extracted from macroalgae as stabilizers in Pickering emulsions.

We hypothesized that polyphenols extracted from *A. nodosum* could be combined with chitosan to increase its dual wettability for preparation of enhanced stable Pickering emulsions by LBL electrostatic deposition technique. For this purpose, this work investigates the effect of multiple parameters (chitosan: polyphenols ratio, chitosan concentrations, oil-phase ratios, pH and NaCl concentrations) on the emulsion characteristics (droplet size and distribution), droplet morphology, and stability of Pickering emulsions. Fourier transform infrared spectroscopy (FTIR), confocal scanning laser microscopy (CLSM), scanning electron microscopy (SEM), contact angle, and atomic force microscopy (AFM) were also used to characterize the binding mode of chitosan and macroalgal polyphenols in co-stabilized Pickering emulsions.

2. Materials and methods

2.1. Biological materials and chemical reagents

Polyphenol extracts were generated from the brown macroalgal *Ascophyllum nodosum* purchased from the company Qingdao Mingyue (Qingdao, Shandong, China). The biomass was processed by ultrasound-assisted enzyme extraction and purified further by removing the fraction soluble in *n*-hexane from the crude extract by liquid-liquid partition, and collecting the polyphenol compounds insoluble in water and soluble in ethyl acetate (Meng et al., not published yet). Further characteristics of these extracts include total polyphenol contents (TPC) of 73.85 g phloroglucinol equivalents (PGE)/100 g dry weight (DW), and antioxidant activities of 104.13 g ascorbic acid equivalents (ACE)/100 g DW when measuring their ABTS scavenging activity, 101.92 g ACE/100 g DW in the case of DPPH radical scavenging activity and 118.17 g Trolox equivalents (TE)/100 g DW when measuring their ferric reducing antioxidant power (FRAP).

The main chemicals used include low molecular weight (MW) chitosan (MW = 50–190 kDa, deacetylation degree = 75–85 %), Folin-Ciocalteu reagent, 2,2′-azino-bis (3-ethylbenzothiazoline-6-sulfonic acid) (ABTS), ascorbic acid, 1,1-diphenyl-2-picrylhydrazyl (DPPH), 2,5,7,8-tetramethylchroman-2-carboxylic acid (Trolox), 2,4,6-tri (2-pyridyl)-*s*-triazine (TPTZ), all purchased from Sigma-Aldrich, Inc. (St. Louis, MO, USA). Corn oil was purchased from Arawana (Beijing, China). Acetic acid, sodium acetate, ferric chloride and other reagents used in this study were of analytical grade and purchased from Beijing Chemical Reagents Co. (Beijing, China).

2.2. Preparation of chitosan and polyphenol solutions

Chitosan solutions (1 %, w/v, pH = 3) were prepared referred to the method described by Lv et al. (2020) with slight modifications. Briefly, chitosan powder was dissolved in distilled water by means of adjusting pH to 3 by slowly adding 1 M HCl under magnetic stirring at 300 rpm for 4 h and then incubated overnight at room temperature. Polyphenol solutions (1 %, *w/v*, pH = 3) were prepared using an ultrasonic bath (SK8210HP, Kudos, Shanghai, China) at 53 kHz, 500 W, 25 °C for 15 min to disperse polyphenols in an aqueous HCl solution.

2.3. ζ-Potential measurements

The ζ-potential of chitosan and polyphenol solutions (0.01 %, *w/v*) was tested at pH ranging from 3 to 9 and the chitosan-polyphenol solutions at different ratios of chitosan: polyphenols were measured at pH 6. Measurements were performed at 25 °C using Zetasizer Nano ZS (Malvern Instruments Ltd., Malvern, Worcestershire, UK) as described by Chen et al. (2018) with slight modifications. Solutions were equilibrated for 120 s and the ζ-potential values were calculated by the Helmholtz-Smoluchowski Equation.

2.4. Preparation of emulsions

Pickering emulsions were prepared by LBL electrostatic deposition method as mentioned by Jo et al. (2021) with slight modifications. As shown in table S1, the effect of each individual factor was analysed in a sequential manner while keeping the remaining factors at fixed conditions as follows: (1) different chitosan: polyphenol ratio (1:0, 12.2:1, 9.5:1, 6.8:1, 4.1:1 and 1.4:1, w:w) were tested in the emulsions at fixed conditions at 0.2 % (w/v) chitosan, 20 % (*v*/v) oil-phase ratio, pH 3 and 0 mM NaCl; (2) several chitosan concentrations (0.2, 0.3, 0.4 and 0.5 %, w/*v*) were assayed in the emulsions at fixed 9.5:1 (w:w) ratio chitosan: polyphenols, 20 % (v/v) oil-phase ratio, pH 3 and 0 mM NaCl; (3) variable oil-phase ratios (5, 10 and 20 %, v/v) keeping the emulsions at fixed 9.5:1 (w:w) ratio chitosan: polyphenols, 0.5 % (w/v) chitosan, pH 3 and 0 mM NaCl; (4) pH variations (3, 5, 6, 7 and 9) were generated keeping the other parameters fixed at 9.5:1 (w:w) ratio chitosan: polyphenols, 0.5 % (w/v) chitosan, 20 % (v/v) oil-phase ratio and 0 mM NaCl; and (5) multiple NaCl concentrations (0, 10, 20, 40, 60 and 100 mM) were assayed in emulsion at 9.5:1 (w:w) ratio chitosan: polyphenols, 0.5 % (w/v) chitosan, 5 % (v/v) oil-phase ratio and pH 6.

The process for the generation of the emulsions is described in Fig. 1. Briefly, chitosan solutions were diluted to chitosan concentration as 0.4, 0.6, 0.8, or 1.0 % (w/v), while the polyphenol solution was diluted with water according to the desired concentration. 0.1 M HCl or NaOH solutions were added to chitosan and polyphenol solutions to adjust pH to 3, 5, 6, 7, or 9, NaCl crystals were added to chitosan solutions until the NaCl concentration were 0, 20, 40, 80, 120, or 200 mM. 50 mL of chitosan solution were mixed with oil *v*olumes ranging from 5 to 20 mL to achieve 5, 10, or 20 % (v/v) oil-phase ratios and homogenized at 10,000 rpm for 1 min using I25 High-speed homogenizer (IKN Co., Shanghai, China) to form crude emulsions. These crude emulsions were homogenized using high-pressure homogenizer (D-3 L, PhD Technology LLC, USA) at 60 MPa for 3 cycles to generate the primary Pickering emulsion. Volumes of 45 mL, 40 mL, or 30 mL of polyphenol solutions were slowly added to achieve 5, 10, or 20 % (*v*/v) oil-phase ratio, respectively. The mixtures were homogenized in high-speed homogenizer (10,000 rpm, 1 min), followed by 3 additional cycles in the high-pressure homogenizer at the previously mentioned conditions.

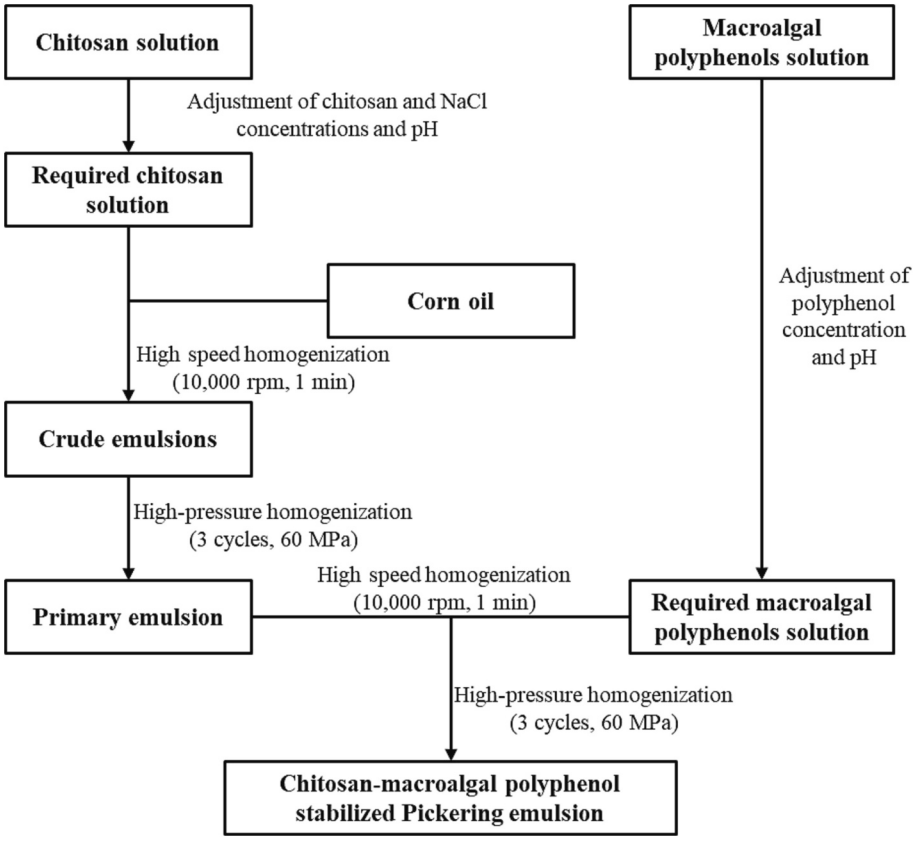

Fig. 1. Preparation procedures of chitosan-macroalgal polyphenol stabilized Pickering emulsion.

2.5. Droplet size and distribution measurements

The size and distribution of droplets were measured using laser particle size analyser (Bettersizer 2000, Dandong Baite Instrument Co., Ltd., Dandong, Liaoning, China) according to the method described by Khan et al. (2014) with slight modifications. Briefly, 0.5 mL of emulsion were diluted in 400 mL of deionized water. The relative refractive index of the emulsion was taken as 1.107, corresponding to the ratio of the refractive indices of corn oil and deionized water of 1.472 and 1.33, respectively. Volume moment mean ($D_{[4,3]}$, μm), surface area moment mean ($D_{[3,2]}$, μm), specific surface area (SSA, m^2/g), percentage of droplets with <10 μm diameter (L10,%) and droplet size distribution were measured.

2.6. Optical microscopic images of emulsions

The microscopic observation of the emulsions were performed as indicated by Chen et al. (2019). Fresh emulsions were diluted 10 times and 20 μL of each mixture were placed on slides and covered with glass (Citotest labware manufacturing Co., LTD, Haimen, Jiangsu, China). Optical microscope equipped with a 40× magnification objective lens and a 10× magnification eyepiece (CX41, Olympus Corporation, Tokyo, Japan) was used to evaluate the microscopic morphology of the droplets and the images were taken using CCD camera (EOS 450D, Canon, Japan).

2.7. Macroscopic observation of emulsion

The macroscopic observation of the emulsions were performed as indicated by Zhu et al. (2021) with some modifications. Briefly, 7 mL of fresh emulsions were pipetted into a 10 mL clear glass bottles and sealed. After 12 h of storage at room temperature, the macroscopic state of the emulsion was recorded by CCD camera (EOS 450D, Canon, Japan).

2.8. Emulsion physical stability (EPS)

EPS was evaluated by the method as described by Kasiri and Fathi (2018). 10 mL of fresh emulsion were centrifuged at 3000 *g* for 15 min at 4 °C. Leakage of the oil-phase at the top and/or water phase separated at the bottom from the emulsions were measured and used to calculate EPS based on the following equation:

$$EPS\ (\%) = (Final\ emulsion\ volume\ (mL)/Initial\ emulsion\ volume\ (mL)\ ) \times 100 \quad (1)$$

2.9. Characterization of chitosan stabilized Pickering emulsion (CPE) and chitosan-macroalgal polyphenol stabilized Pickering emulsion (CPPE)

CPE and CPPE were prepared as described in the Section 2.4 at chitosan concentration of 0.5 % (w/v), 5 % (v/v) oil-phase ratio, pH 6 and 0 mM NaCl, with the ratio of chitosan: polyphenol of 1:0 for CPE and 9.5:1 for CPPE.

2.9.1. Multiple light scattering stability analyses

Multiple light scattering stability analyses were performed as indicated by Cai et al. (2020) with slightly modifications using Turbiscan Lab instrument (Formulaction Co., L'Union, France). Briefly, the measuring cell was filled with 20 mL of CPE or CPPE, performing the measurement at 50 °C during 6 h. The Turbiscan stability index (TSI) was calculated using the Turbiscan Tower software (Formulaction Co., L'Union, France) using the following equation:

$$TSI = \sum_i \frac{\sum_h |scan_i(h) - scan_{i-1}(h)|}{H} \quad (2)$$

where $scan_i(h)$ is the average backscattering at each time (i) of measurement, $scan_{i-1}(h)$ is the average backscattering for the time (i-1) of

measurement, and H is the height of the sample.

2.9.2. FTIR analyses

FTIR analyses were performed as described by Daoud et al. (2019) with slight modifications. Briefly, 20 μL of fresh Pickering emulsion samples were spread directly on the crystal surface of the FTIR spectrometer and the absorbance spectrum was collected. The FTIR spectra at IR ranges of 600 and 4000 cm^{-1} with a resolution of 2 cm^{-1} were recorded using Tensor 27 FTIR spectrometer (Bruker, Karlsruhe, Germany). The crystal was cleaned with pure ethanol between measurements.

2.9.3. CLSM

The microstructure of the emulsions were visualised as indicated by Hu et al. (2020) with slight modification using confocal scanning laser microscope TCS SP8, with 63 × objective lens (Leica Microsystems, Heidelberg, Germany). Briefly, 1 mL emulsions were stained with 50 μL of a blended fluorescent colorant solution consisting of FTIC (1 mg/mL) and Nile Red (1 mg/mL) for 1 h. The dyed samples were diluted 10 times and 20 μL of diluted samples were carefully transferred for observation. The autofluorescence of polyphenols was visualised at an excitation wavelength of 405 nm (Flores-Molina et al., 2016). FITC-labelled chitosan was observed at an excitation wavelength of 488 nm (Atarian et al., 2019). Using Nile red staining the oil-phase of emulsions were visualised at excitation wavelength of 514 nm (İlyasoğlu et al., 2019). The optical resolution of the digital images was 2048 pixels × 2048 pixels.

2.10. Characterization of interfacial layer of CPE and CPPE

2.10.1. Interfacial layer separation

The extraction of the interfacial layer of CPE and CPPE was based on the methods described by Wang et al. (2022) with slightly modifications. CPE and CPPE were centrifuged (10,000 *g*, 20 min), 10 volumes of *n*-hexane were added and the mixtures were heated (65 °C, 30 min) to remove oil. The mixtures were then centrifuged (10,000 *g*, 20 min) to remove the *n*-hexane fraction, and collect the interfacial layer that was then freeze-dried, vacuum sealed and preserved at −20°Cfor further experiments.

2.10.2. SEM

The morphology and shape of the interfacial layer of CPE and CPPE were observed by SEM using a S-3400 scanning electron microscope (Hitachi, Ltd., Tokyo, Japan) at 10 kV. The freeze-dried samples were adhered to a conductive carbon tape, and gold particles were deposited on the surface with a sputter coater under vacuum to avoid charging effects before the SEM observations.

2.10.3. AFM

Stabilizer of CPE and CPPE were evaluated with AFM (NX10, Park Co., Ltd., Korea) following the method described by Mudugamuwa Arachchige et al. (2021) with slightly modifications. Briefly, 10 μL dispersed interfacial layer in deionized water (10 μg/mL) were dipped on a freshly cleaved mica sheets and dried overnight. The sheets were bound to a magnetic stainless-steel disk and scanned.

2.10.4. Contact angle

Contact angles of the interfacial layer of CPE and CPPE were obtained with a DSA 30 Contact Angle System (with goniometer equipped with a system of drop shape analysis, Krüss, Germany).

2.10.5. TPC and antioxidant activities of the interfacial layer of CPE and CPPE

The interfacial layers of these two emulsions were dispersed into deionized water in ultrasonic bath (0.1 mg/mL) for the subsequent analyses.

2.10.5.1. TPC.

TPC measurements were performed as indicated by Meng, Mu, et al. (2022). In brief, 1 mL of 10 % (v/v) Folin-Ciocalteu reagent was added to 0.5 mL of sample or standard and incubated at 30 °C in dark for 30 min. 2 mL of a Na_2CO_3 solution (10 %, w/v) were then added to the mixtures and incubated for additional 30 min following the aforementioned conditions. The absorbance of the samples was determined at 770 nm using spectrophotometer (U-3010, Tokyo Hitachi Co., Ltd., Tokyo, Japan), TPC was expressed as g PGE/100 g interfacial layer.

2.10.5.2. ABTS scavenging activity.

ABTS values were determined following the method as described by Meng, Liu, et al. (2022). Briefly, 1 mL of sample mixtures were mixed with 2 mL of ABTS working solution and then incubated for 6 min in dark conditions. The absorbance was measured at 734 nm by spectrophotometer, ABTS values were expressed as mg ACE/g interfacial layer.

2.10.5.3. DPPH scavenging activity.

DPPH scavenging activity of the samples was determined as described by Zhu et al. (2022) with slight modifications. 2 mL of samples were mixed with equal volume of DPPH working solution (0.2 mM) for 30 min in dark conditions. Absorbance of mixtures was recorded at 517 nm using spectrophotometer, DPPH *v*alues was expressed as mg ACE/g interfacial layer.

2.10.5.4. FRAP.

FRAP determinations were performed based on the method as described by Luo et al. (2021) with some modifications. FRAP solution was prepared by mixing 10 mM TPTZ solution in 40 mM HCl, 20 mM $FeCl_3$ solution in 0.3 M acetate buffer (pH 3.6) and 0.3 M acetate buffer (pH 3.6) at a ratio 1:1:10 (*v*:v:v). 1 mL of sample solutions were mixed with 2 mL FRAP solution previously heated to 37 °C for 30 min. The mixtures were incubated for further 30 min at 37 °C. The absorbance of the samples was read at 593 nm using spectrophotometer. FRAP was expressed as mg TE/g interfacial layer.

2.11. Statistical analyses

All the measurements were performed in triplicate and the results expressed as mean ± standard deviation (SD). One-way ANOVA and Duncan's multiple range tests were conducted to identify differences inside each treatment group using SPSS version 27.0 (IBM, Armonk, NY, USA). In all cases, the criterion for statistical significance was $P < 0.05$.

3. Results and discussion

3.1. Effects of pH on the ζ-potential of chitosan and polyphenol solutions

ζ-potential of the chitosan solutions decreased with the increase of pH value (Fig. 2A). At pH 3, the ζ-potential of the chitosan solution was the highest (50.2 ± 1.8 mV), decreasing at higher pH until reaching its lowest value (2.6 ± 0.6 mV) at pH 9. The ζ-potential of the chitosan solutions were always positive at pH ranging from 3 to 9, with aggregation appreciated in the solution at pH > 7 following the rapid decrease of ζ-potential. Similar behavior was appreciated at pH 7 in chitosan solutions in previous studies (Chang et al., 2015). The ζ-potential of macroalgal polyphenol solutions at different pH were represented in Fig. 2B. The ζ-potential had negative when analysed at the same pH ranges as chitosan. At pH 3, the ζ-potential of the polyphenol solution was the highest (−24.8 ± 1.4 mV), and these values decreased at increasing levels of pH reaching the lowest values at pH 9 (−41.2 ± 0.9 mV). Interactions of chitosan with other polymers has been mainly linked to the electrostatic forces between positively charged chitosan and negatively charged polymers, as well as the formation of hydrogen bonds, van der Waals forces and hydrophobic interactions (Sharkawy et al., 2020). Thus, the differences in ζ-potential appreciated between chitosan and polyphenols indicated the potential for interaction

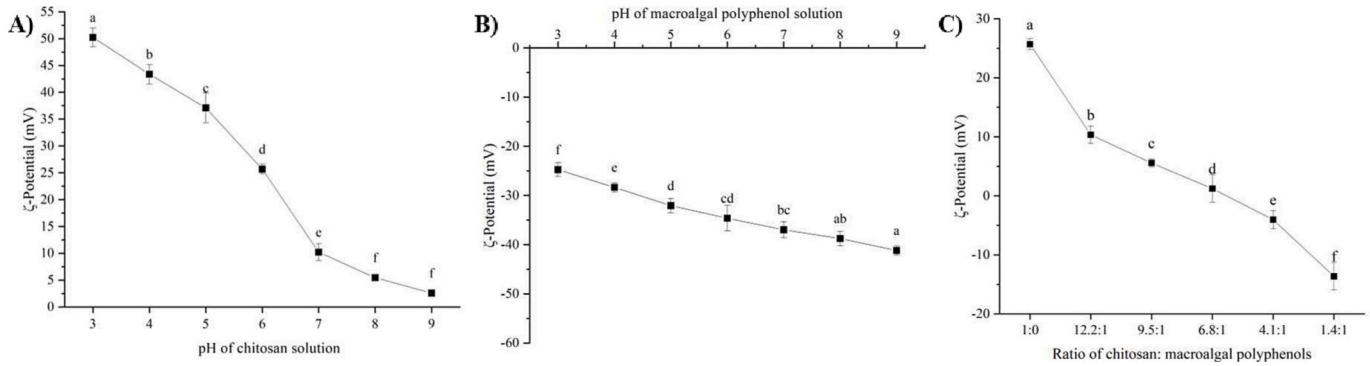

Fig. 2. ζ-Potential of (A) chitosan solutions and (B) macroalgal polyphenol solution at different pH (3–9), (C) mixtures of chitosan-polyphenol at multiple chitosan: polyphenol ratios (1:0 to 1.4:1) at pH 6. Different letters indicate statistical differences ($P < 0.05$) in ζ-potential between the different conditions inside each figure.

between these two polymers could be useful when generating composites. As shown in Fig. 2C, as increased of the ratio of chitosan: polyphenol from 1:0 to 1.4:1, negatively charged macroalgal polyphenol combined with positively charged chitosan, while ζ-potential in the chitosan-polyphenol solution mixtures decreased from 25.68 mV (1:0) to −13.63 mV (1.4:1) at pH 6.

3.2. Macroscopic observations

Images of emulsions generated by analysing the effect of different chitosan: polyphenol ratios, chitosan concentrations, oil-phase ratios, pH values, and NaCl concentrations while keeping the other parameters of emulsion fixed were compiled in Fig. 3. The macroscopic evaluation of all these emulsions revealed that the formulations were all stable within 12 h after formation, with no leakages of either oil or water phases or aggregation of droplets. This finding was similar to previous reports using chitosan in Pickering emulsion combined with other natural compounds, including carboxymethyl cellulose, zein and tripolyphosphate (Shah, Xu, & Mráz, 2021; Wang et al., 2016; Zhu et al., 2021). These emulsions do not rapidly separate into oil and water phases during short-term storage.

3.3. Distribution of droplets

The effect of the variation of individual parameters on the droplets size and microscopic distribution of emulsions are summarised in Table S2 and Fig. 4, respectively. $D_{[4,3]}$ were the highest (10.47 μm) and lowest (2.42 μm) at chitosan: polyphenol ratios of 1:0 and 1.4:1, respectively. However, $D_{[3,2]}$ was the highest (1.68 μm) at chitosan: polyphenol ratio of 1.4:1, while the minimum values (1.49 μm) were appreciated at 6.8:1 chitosan: polyphenols ratio. As shown in Fig. 4A, ratios of chitosan: polyphenols of 9.5:1 had the best droplet morphology. At chitosan: polyphenols ratio of 12.2:1 and 1:0, the content of polyphenols was insufficient to effectively interact with chitosan and form a stable oil-water interface layer, resulting in irregular droplet shapes. Droplets at chitosan: polyphenol ratios of 6.8:1, 4.1:1 and 1.4:1 had a tendency to aggregate that can be attributed to the excessive addition of negative charges and changes in the charge of the droplets surface, resulting in flocculation and reduced stability (Klinkesorn, 2013). In the case of chitosan concentrations, $D_{[4,3]}$ and $D_{[3,2]}$ had a decreasing trend with the addition of chitosan as seen in Fig. 4B, while SSA showed an opposite behavior. These results could be attributed to the increased number of particles that will ultimately lead to larger interfacial area coverage and the formation of small droplet sizes (Mwangi et al., 2016). Similarly, other studies appreciated that an increase in chitosan

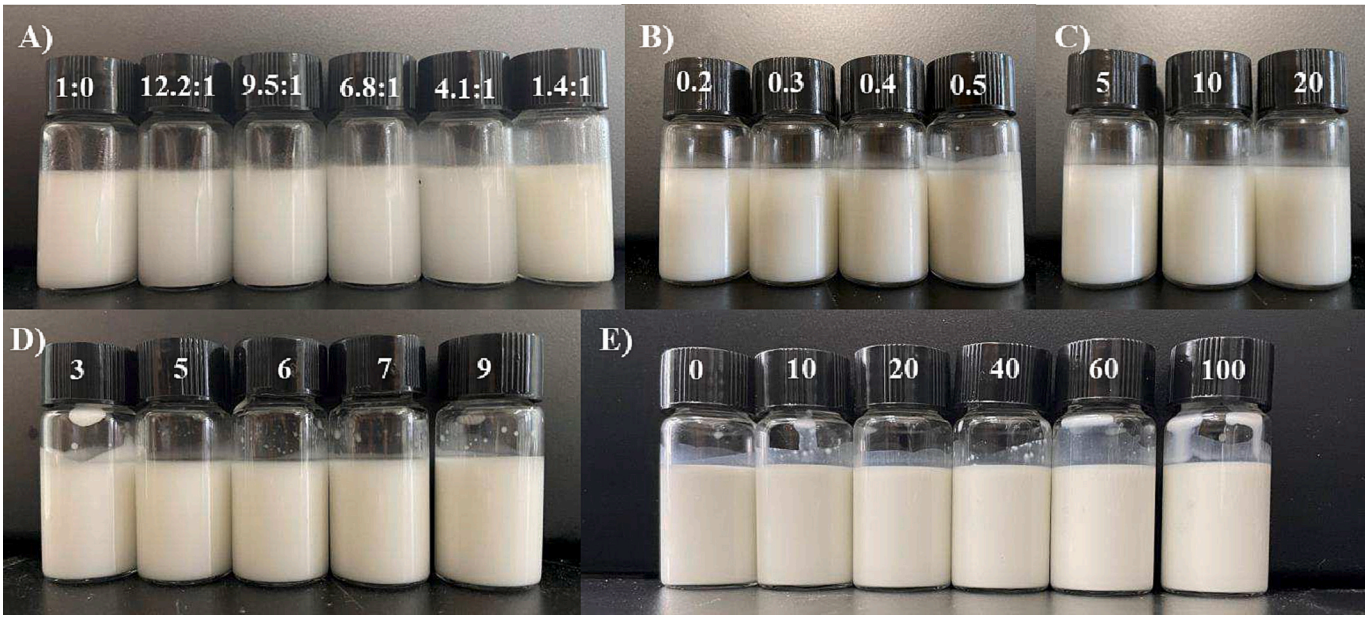

Fig. 3. Macroscopic observation of emulsions at different (A) ratio of chitosan: polyphenols (1:0–1.4:1), (B) chitosan concentrations (0.2–0.5 %, w/v), (C) oil-phase ratios (5–20 %, v/v), (D) pH values (3–9), and (E) NaCl concentrations (0–100 mM).

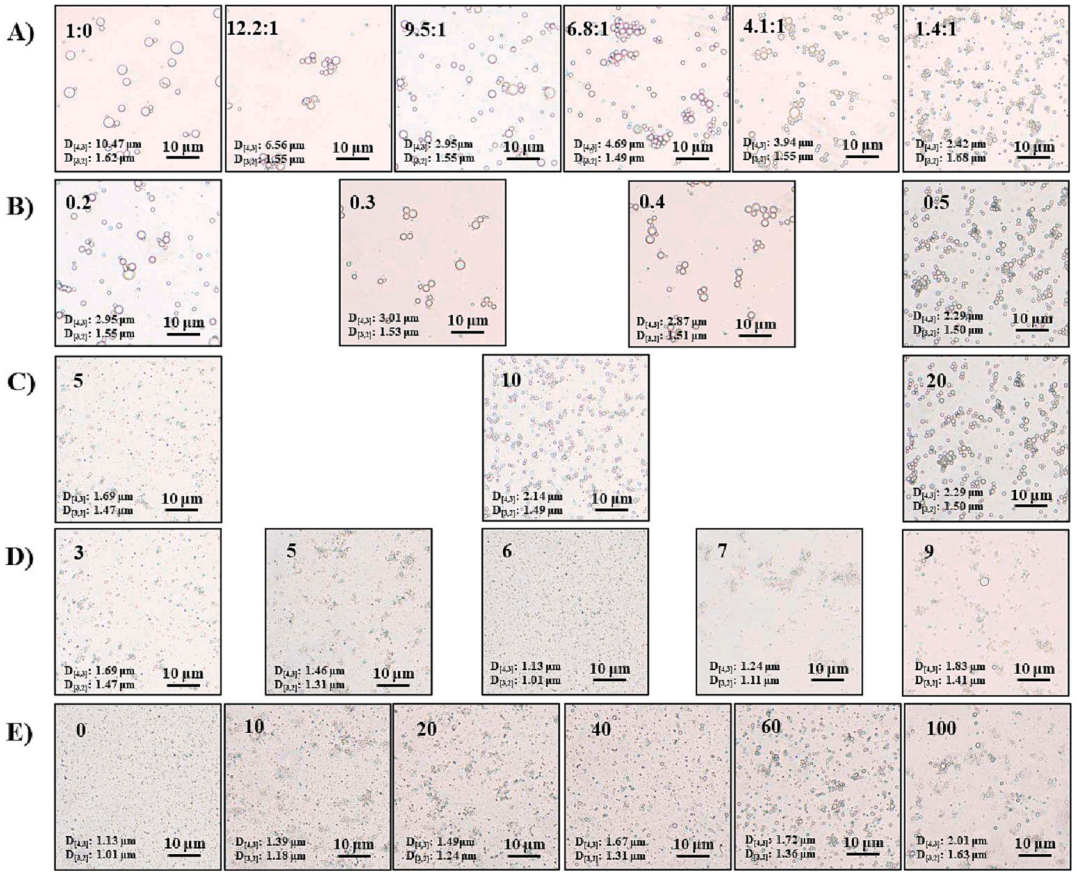

Fig. 4. Microscopic images of emulsions at different (A) ratio of chitosan: polyphenols (1:0–1.4:1), (B) chitosan concentrations (0.2–0.5 %, *w/v*), (C) oil-phase ratios (5–20 %, *v*/v), (D) pH values (3–9), and (E) NaCl concentrations (0–100 mM). The scale bars of each image represent 10 μm.

concentrations in Pickering emulsions resulted in oil fragmentation and small droplets that were less prone to aggregation (Li & Xia, 2011). With the increase of the oil-phase ratio, the D[4,3] and D[3,2] of the emulsions increased, being this result in agreement with the microscopic images of Fig. 4C. Previous studies also appreciated this phenomenon, reporting that increased oil-phase ratio leads to a relative decrease of the concentration of stabilizer molecules at the O/W interface (Sharkawy et al., 2020). In addition, bridging flocculation appeared in the emulsions at 20 % oil ratio, indicating that the concentration of the emulsion stabilizer was not sufficient to stabilize its droplets. Emulsions at 5 % oil ratio had the best droplet distribution. As presented in Fig. 4D, when pH increased from 3 to 6, the particle size of the emulsion droplets decreased, and the emulsions reached the smallest droplet size at pH 6. Emulsions generated at pH 6 had the lowest $D_{[4,3]}$ (1.13 μm), $D_{[3,2]}$ (1.01 μm) and the highest SSA (2.21 m^2/g), which would provide a high potential for their future application as carrier of bioactive ingredients contributing to an increased dispersibility and deformability to allow the carriers to pass through intercellular spaces (Ming et al., 2022). Further increases of pH above 6 resulted in increased droplet sizes, with the emulsions reaching the maximum droplet size at pH 9. At this pH, there is a reduction of the repulsive forces of chitosan-polyphenols polymers, allowing unabsorbed chitosan particles to deposit on the droplets and resulting in larger droplet diameters (Mwangi et al., 2016). In the case of the influence of NaCl on the emulsions, high NaCl concentrations resulted in increases of both $D_{[4,3]}$ and $D_{[3,2]}$ and decreased SSA (Fig. 4E). Previous studies also reported the demand of chitosan adsorbed to the interfacial layer tended to be greater in the presence of salt, leading to larger droplets and thicker interfacial layers (Lundin et al., 2008). Moreover, NaCl could reduce the charge density of chitosan particles (Klinkesorn, 2013), which could lead to decreased stability of the chitosan-polyphenol emulsions. This can also be appreciated in Fig. 4E, showing emulsions with droplets of significantly larger diameters and normally aggregated at NaCl concentrations of 60 mM and 100 mM.

3.4. EPS of chitosan-polyphenol Pickering emulsions

The EPS of emulsions at various chitosan: polyphenol ratios was represented in Fig. 5A. Emulsions had oil-phase leakages after centrifugation at chitosan: polyphenol ratios of 6.8:1, 4.1:1, and 1.4:1, indicating the poor physical stability of these emulsions and the presence of droplet aggregates. Similar results were also reported in emulsions stabilized by rice bran protein and catechins (D. Li et al., 2020). As the concentration of catechins increased, the stability of the emulsions increased initially and then decreased at higher catechin concentrations, resulting in an increased droplet aggregation (D. Li et al., 2020). EPS increased significantly with the increase in chitosan concentrations (Fig. 5B). Previous studies demonstrated that at increased chitosan concentrations, the network structure and viscosity of chitosan in the emulsion increased, providing stronger electrostatic repulsion and steric hindrance forces between the emulsion particles that resulted in reduced spread of the emulsion droplets and increased contact between them (Zhang et al., 2021). EPS of the emulsions increased at high oil-phase ratios (Fig. 5C). Previous studies reported that increased oil-phase ratios contributed to an overall increase of the total volume of the droplets and higher stability of the emulsion droplets as result of crowding effect (Bhutto et al., 2021). EPS also varied at different pH, reaching the minimum of 26.67 and maximum of 95.67 % at pH 9 and 6, respectively (Fig. 5D). As reported by Bhutto et al. (2021), chitosan reaches an equilibrium between protonation and deprotonation at pH 6, resulting

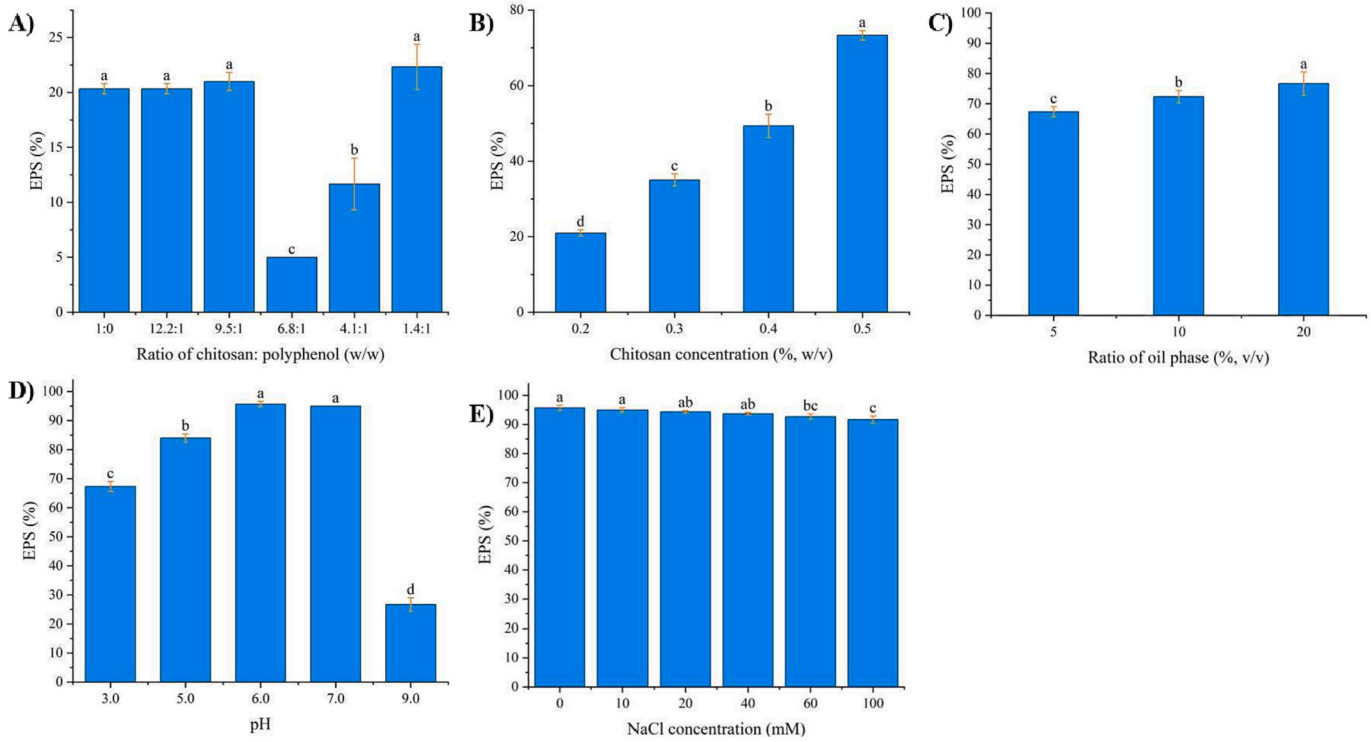

Fig. 5. EPS of emulsions at different (A) ratio of chitosan: polyphenols (1:0–1.4:1), (B) chitosan concentrations (0.2–0.5 %, w/v), (C) oil-phase ratios (5–20 %, v/v), (D) pH values (3–9), and (E) NaCl concentrations (0–100 mM). Different letters inside each figure indicate statistical differences ($P < 0.05$) of EPS between the emulsions.

in the formation of sufficient nanoscale aggregated particles to stabilize the emulsion droplets. Emulsions at pH 3 and 9 had significantly lower EPS than those appreciated at other pH values, which could be attributed to the protonation of the amino groups on the d-glucosamine units of chitosan at low pH, leading to weaker electrostatic repulsion between chitosan polymer chains, higher adsorption at the interface, and ultimately a greater interface coverage (Mwangi et al., 2016). All these effects have been reported to result in increased droplet size of emulsions at high pH values (Sharkawy et al., 2020). In the case of the effect of NaCl, EPS decreased at high NaCl concentrations (Fig. 5E). This effect may be attributed to the increased ionic strength of the solution and enhanced electrostatic shielding effects, that suppress the complexation forces between chitosan and polyphenols and the sites available for interaction between both molecules, leading to a decreased emulsion stability (Aoki et al., 2005; Klinkesorn, 2013; Zhang et al., 2021).

3.5. Characterization of CPE and CPPE

After appreciating the effect of all parameters on chitosan-macroalgal polyphenol Pickering emulsions, the optimum conditions for the preparation of these emulsions were 9.5:1 chitosan: polyphenol ratio (w:w), 0.5 % (w/v) chitosan concentration, 5 % (v/v) oil-phase ratio, pH 6, and 0 mM NaCl concentration. These conditions were used for the preparation of CPE and CPPE to analyse the stability, FTIR, and CLSM to elucidate the type of binding between chitosan and polyphenols in the emulsions, as well as SEM, AFM, contact angle and antioxidant activity of the interfacial layer of CPE and CPPE.

3.5.1. Multiple light scattering stability analysis

Multiple light backscattering measurements were used to evaluate the stability of the emulsions, with high TSI values associated to low stability values in emulsions (Tong et al., 2021). As shown in Fig. 6A, CPE had larger TSI values (2.75) compared to those of CPPE (1.80), indicating the higher stability of the CPPE. Moreover, the backscattering (BS%) of CPE (Fig. 6B) and CPPE (Fig. 6C) during the measurement was used to evaluate their dynamic analysis in unstable processes (Cai et al., 2020). The left side of the horizontal axis of the curve was the bottom of the sample cell, the right side was the top of the sample cell, and the ordinate was the intensity of the backscattered light (BS%). As shown in Fig. 6B, the flocculation of droplets appeared on the top of the emulsion of CPE over time, resulting in changes of BS%, while CPPE (Fig. 6C) did not have these changes, indicating that CPPE had stronger ability to resist droplet flocculation than CPE.

3.5.2. FTIR

FTIR spectroscopy results were summarised in Fig. 7. Comparing FTIR results between CPE and CPPE there were strong broadband O—H stretching changes that shifting from 3244.2 cm^{-1} in CPE to 3223.0 cm^{-1} in CPPE. Moreover, the intensity of the peak of N—H stretching at 3656.9 cm^{-1} in CPE decreased and shifted to 3643.4 cm^{-1} in CPPE. Wavenumber reduction in CPPE compared to CPE may be attributed to the generation of intermolecular hydrogen bonds between chitosan and macroalgal polyphenols (F. Li et al., 2021; Noshad et al., 2016).The characteristic peaks located at 2877.7 cm^{-1} and 1128.3 cm^{-1} correspond to the C—H stretching vibrations and C-O-C asymmetric stretching vibrations of chitosan particles, respectively (Staroszczyk et al., 2014; Yoksan et al., 2010). The wavenumbers of these bonds were the same in both emulsions, indicating that the macroalgal polyphenols did not interact with the backbone structure of chitosan particles. Moreover, the peak position of the amide I band of chitosan particles was significantly shifted from 1629.8 cm^{-1} (CPE) to 1633.7 cm^{-1} (CPPE), while the amide II band was shifted from 1485.1 cm^{-1} (CPE) to 1496.7 cm^{-1} (CPPE), which suggested that macroalgal polyphenols may be involved in electrostatic interactions with the NH_3^+ functional groups of oppositely charged chitosan (Noshad et al., 2016, 2015; Staroszczyk et al., 2014). Overall, based on FTIR analysis, chitosan and macroalgal polyphenols in these emulsions were bound by intermolecular hydrogen bonds and electrostatic interactions.

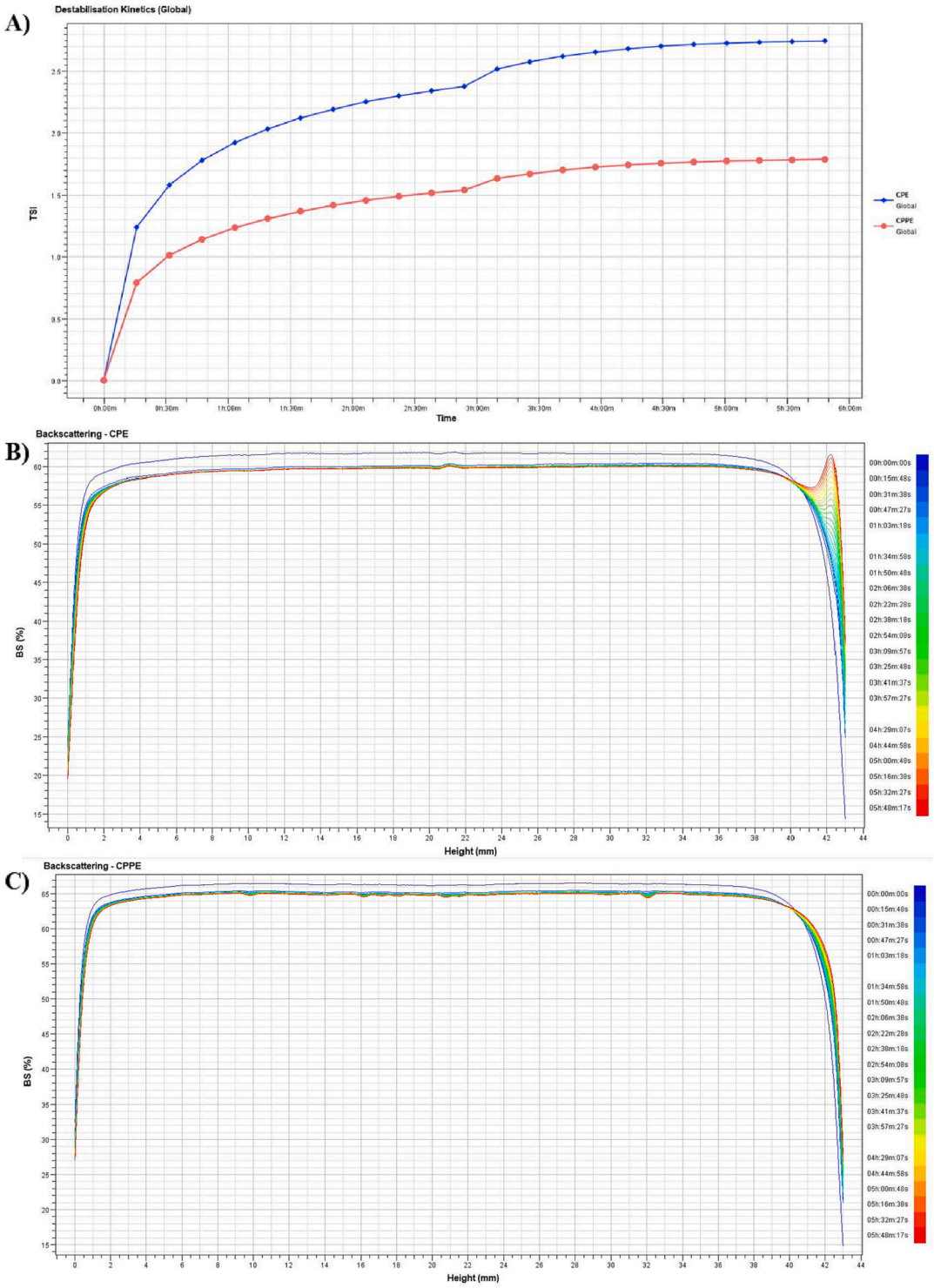

Fig. 6. (A) Turbiscan stability index (TSI) of CPE and CPPE emulsions; and backscattering profiles of (B) CPE and (C) CPPE.

3.5.3. CLSM

Fig. 8 showed CLSM images of CPPE in an optical field (droplets, Fig. 8A), blue fluorescence field (polyphenols, Fig. 8B), red fluorescence field (chitosan, Fig. 8C) and green fluorescence field (corn oil, Fig. 8D), respectively. The distribution of droplets in the emulsion was homogeneous (Fig. 8A), while macroalgal polyphenols (Fig. 8B) and chitosan (Fig. 8C) were dispersed in the continuous phase, as well as chitosan and polyphenols aggregated near the droplets. The distribution of chitosan particles in the dispersed phase and oil-water interface was similar to that of previous reports (Tabatabaei, Rajaei, et al., 2022). The distribution of macroalgal polyphenols was not uniform, and the compounds were mainly concentrated around the droplets, which may indicate that chitosan and macroalgal polyphenols may interact to form a stable structure at the oil-water interface to stabilize emulsion droplets. The uniform oil droplet distribution (Fig. 8D) was similar to that reported in previous studies on caffeic acid-grafted chitosan-stabilized emulsion (İlyasoğlu et al., 2019); however, CPPE had a smaller droplet size compared to that of their reports.

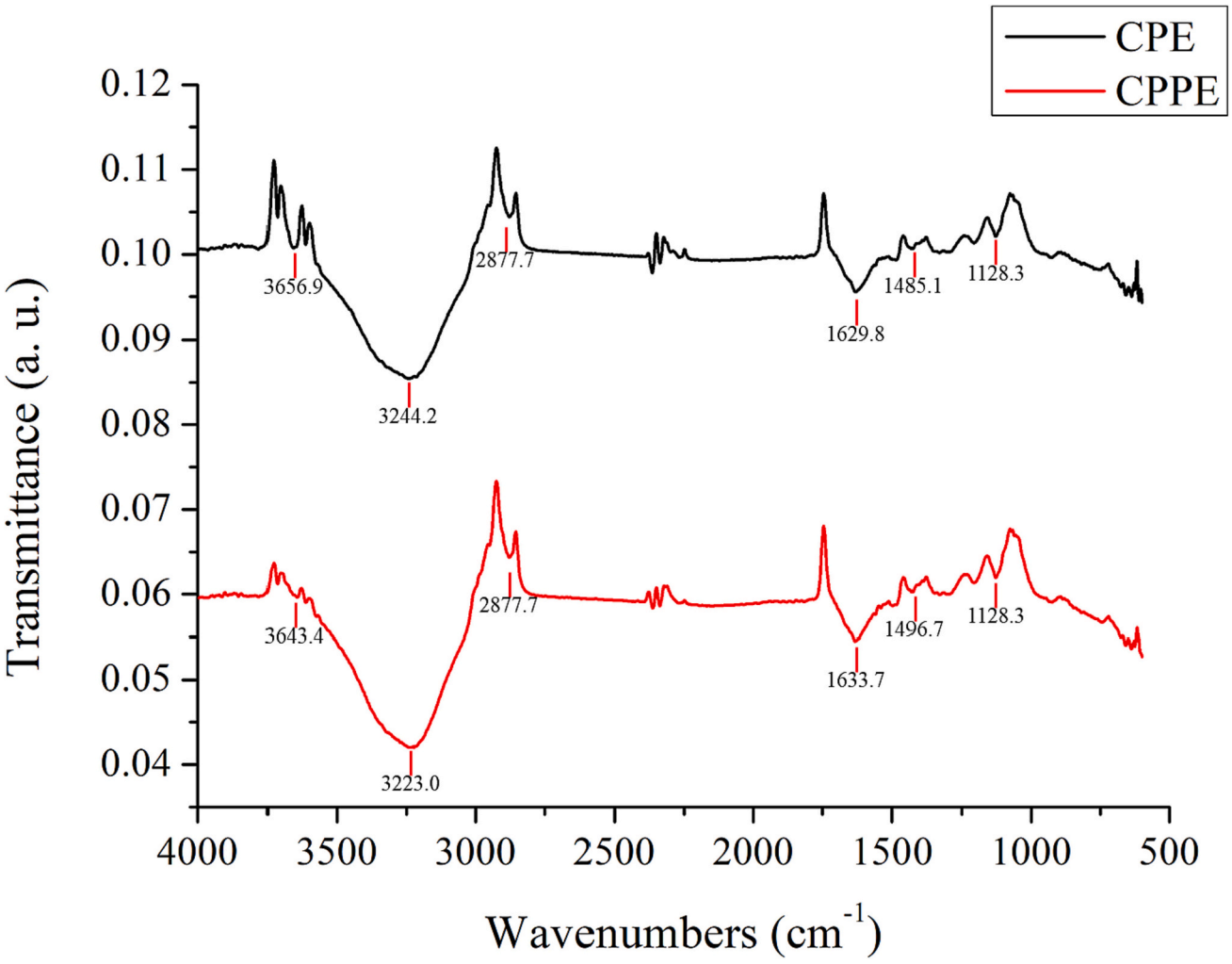

Fig. 7. FTIR spectra of CPE and CPPE.

3.5.4. Contact angle

The wetting properties of the interfaical layer of CPE (Fig. 9A) and CPPE (Fig. 9F) were investigated by determining oil/water three-phase contact angles ($\theta_{o/w}$). Previous studies reported that the excessive hydrophilicity of the chitosan molecules represent a limitation for the use of chitosan particles as stabilizers of Pickering emulsion (Sultan et al., 2022; Tabatabaei, Ebrahimi, & Rajaei, 2022). The $\theta_{o/w}$ of the interfacial layer of CPPE was 87.8°, exhibiting higher hydrophobicity compared to CPE (69.0°). As the contact angle of the stabilizer approached 90°, its ability to stabilize Pickering emulsions was more pronounced (F. Li et al., 2021). Therefore, the addition of macroalgal polyphenols present in the interfacial layer of CPPE contributed to improve the dual wettability of chitosan and improved the performance of this molecule as stabilizer in Pickering emulsions.

3.5.5. SEM

SEM was conducted to achieve a detailed shape and morphological information of CPE and CPPE interfacial layer (Fig. 9 B, C in the case of CPE and Fig. 9 G, H for CPPE). The interface layers of CPE and CPPE were both composed of spherical particles, similar to previous studies characterizing chitosan-based particles (Meng, Liu, et al., 2022; Tabatabaei, Rajaei, et al., 2022). In addition, the interfacial layer of CPPE has tighter inter-particle connections compared to that of CPE, which was also observed in previous studies analysing chitosan-ascorbyl palmitate nanoparticles (Yoksan et al., 2010). The results of SEM showed that chitosan and macroalgal polyphenols could be combined in the oil-water interface layer of Pickering emulsion to produce a more compact structures.

3.5.6. AFM

In order to further demonstrate the interaction force and aggregation between chitosan and macroalgal polyphenols, and the morphology of the interfacial stabilizer of CPE (Fig. 9D, E) and CPPE (Fig. 9I, J) was observed by AFM. In the images, the particles of the CPE and CPPE interface layers were spherically shaped and homogeneously dispersed, and in the case of CPPE particles had larger height and diameter than those of CPE, demonstrating the complexity of the chitosan and macroalgal polyphenols aggregates. Similar AFM resuls were also appreciated in Pickering emulsions stabilized by OSA-modified starch/chitosan composite particles (Yan et al., 2019).

3.5.7. Antioxidant activities

As shown in Fig. 10, the interfacial layer of CPPE had higher antioxidant activity than that of CPE. Polyphenols had been previously reported to enhanced the antioxidant activity when used as stabilizers of Pickering emulsions, such as chitosan-gallic acid composites (Xie et al., 2014) and chitosan-caffeic acid composites (İlyasoğlu et al., 2019). The TPC of CPPE were 32.01 mg PGE/g interfacial layer, resulting in incresead ABTS scavenging activity (34.88 mg ACE/g interfacial layer), DPPH scavenging activity (44.51 mg ACE/g interfacial layer) and FRAP (43.35 mg TE/g interfacial layer) compared to those of CPE (ABTS scavenging activity of 2.61 mg ACE/g interfacial layer, DPPH

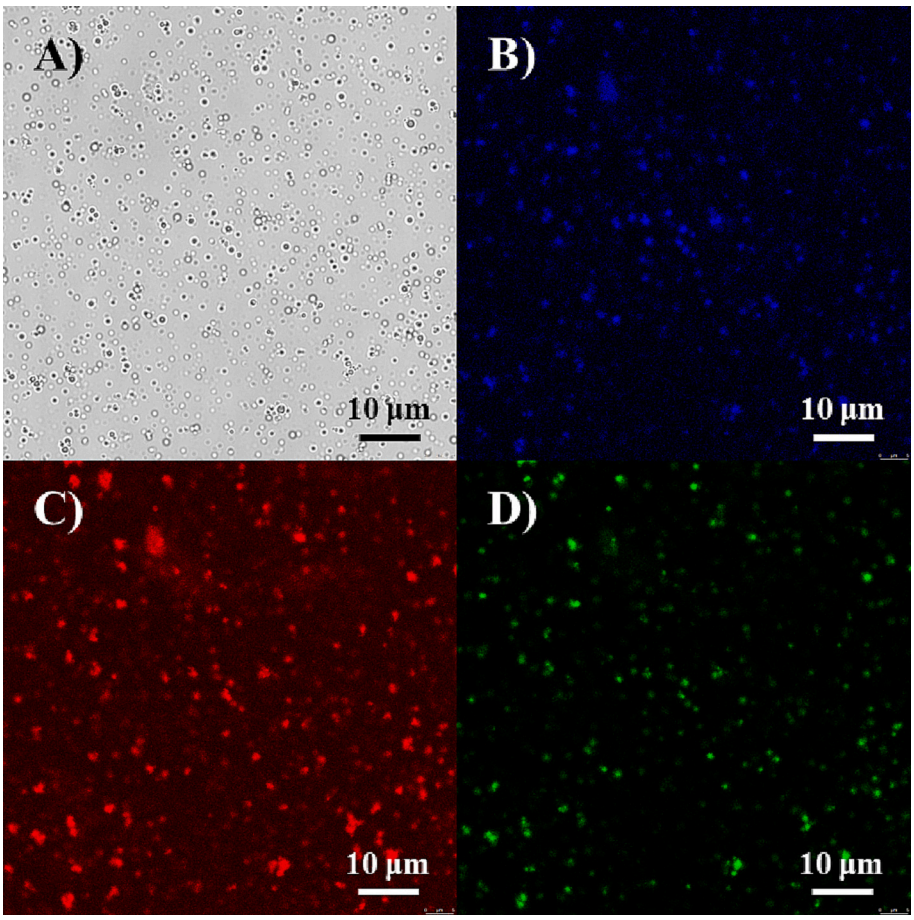

Fig. 8. CLSM images of CPPE using (A) optical microscopy, (B) blue fluorescence field for the visualization of polyphenols, (C) red fluorescence field for the visualization of chitosan; and (D) green fluorescence field for the visualization of corn oil. The scale bars of the images represent 10 μm. (For interpretation of the references to color in this figure legend, the reader is referred to the web version of this article.)

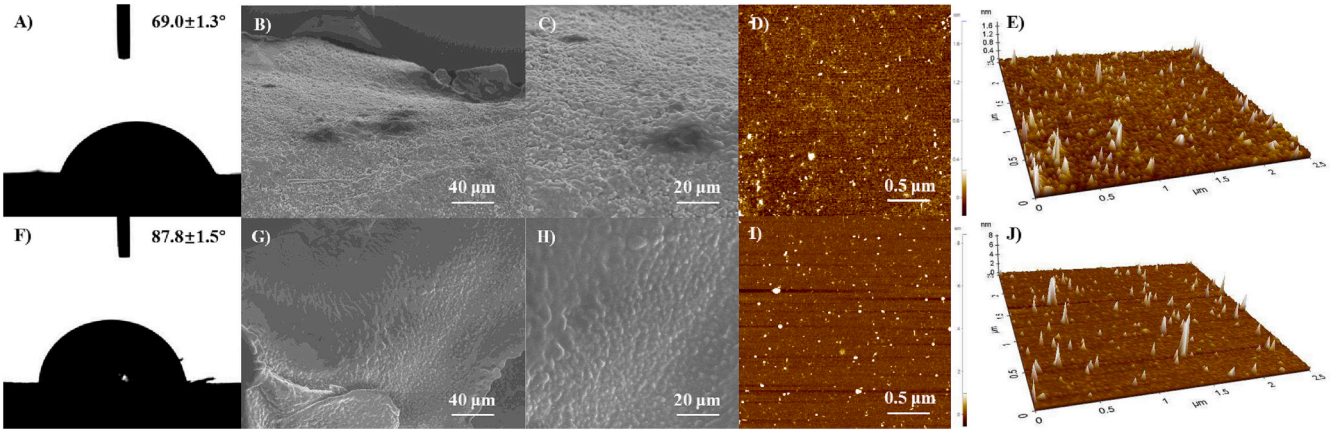

Fig. 9. Contact angle of (A) CPE and (F) CPPE; SEM images of (B, C) CPE and (G, H) CPPE; AFM images of CPE ((D) height and (E) 3D images) and CPPE ((I) height and (J) 3D images) interfacial layer.

scavenging activity of 3.10 mg ACE/g interfacial layer and FRAP of 2.57 mg TE/g interfacial layer). This study demonstrated that macroalgal polyphenol can also provide a significant enhancement of the antioxidant activity of the stabilizer and confer the potential to improve the oxidative stability in these emulsions.

4. Conclusion

This study optimized the preparation of novel chitosan-macroalgal polyphenol Pickering emulsions by analysing the effect of single factors chitosan: polyphenols ratio (1:0–1.4:1), chitosan concentration (0.2–0.5 %, w/v), ratio of oil-phase (5–20 %, v/v), pH (3–9) and NaCl concentration (0–100 mM) on the emulsions generated by LBL electrostatic deposition technology. The effect of all these parameters on the

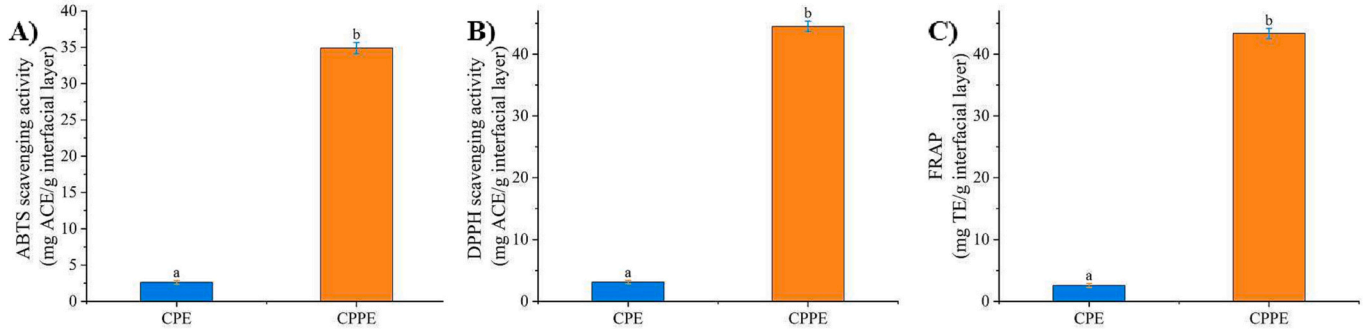

Fig. 10. Anitioxidant activities (A) ABTS, (B) DPPH, and (C) FRAP of interfacial layer of CPE and CPPE.

emulsion properties (EPS, morphology and particle size distribution) concluded that emulsions with 9.5:1 chitosan: polyphenols ratio (w:w), 0.5 % (w/v) of chitosan concentration, 5 % (v/v) oil-phase ratio, pH 6, and 0 mM NaCl had optimal emulsion properties, including the highest EPS and SSA, for their application as delivery systems of bioactive compounds. In addition, the results of multiple light scattering, CLSM, contact angle, SEM, AFM and antioxidant activity analysis of the interfacial layer of CPPE compared to those CPE demonstrated that chitosan and macroalgal polyphenols could be tightly bound at the oil-water interface of Pickering emulsions through electrostatic interactions and hydrogen bonds, improving their dual wettability of chitosan particles. Moreover, the addition of polyphenols improved the stability and antioxidant power of the emulsions. These results will contribute to the development of delivery systems based on chitosan and macroalgal polyphenols for the protection of hydrophobic bioactive compounds with useful applications in the functional food and pharmaceutical industries. Furthermore, this study could also contribute to provide innovative uses of polyphenols extracted from macroalgae, beyond those of the inclusion of these molecules in food formulations as natural antioxidants for the development of functional foods.

Statement of informed consent, human/animal rights

No conflicts, informed consent, or human or animal rights were applicable to this study.

CRediT authorship contribution statement

Weihao Meng: References collection, Software, Validation, Visualization and Writing–original draft and editing.

Hongnan Sun: Methodology, Supervision, and Writing-review and editing.

Taihua Mu: Conceptualization, Supervision, and Writing-review.

Marco Garcia Vaquero: Supervision, and Writing-review.

Declaration of competing interest

The authors have no conflicts of interest to declare.

Data availability

Data will be made available on request.

Acknowledgements

Weihao Meng is currently in receipt of a PhD Scholarship within the joint collaborative PhD programme between UCD and GSCAAS. This study is funded by the Science and Technology Innovation Project of Chinese Academy of Agricultural Sciences (CAAS-ASTIP-202X-IFST).

Appendix A. Supplementary data

Supplementary data to this article can be found online at https://doi.org/10.1016/j.carbpol.2022.120256.

References

Aoki, T., Decker, E. A., & McClements, D. J. (2005). Influence of environmental stresses on stability of O/W emulsions containing droplets stabilized by multilayered membranes produced by a layer-by-layer electrostatic deposition technique. *Food Hydrocoll., 19*(2), 209–220. https://doi.org/10.1016/j.foodhyd.2004.05.006

Atarian, M., Rajaei, A., Tabatabaei, M., Mohsenifar, A., & Bodaghi, H. (2019). Formulation of Pickering sunflower oil-in-water emulsion stabilized by chitosan-stearic acid nanogel and studying its oxidative stability. *Carbohydrate Polymers, 210* (September 2018), 47–55. https://doi.org/10.1016/j.carbpol.2019.01.008

Bai, Y., Sun, Y., Gu, Y., Zheng, J., Yu, C., & Qi, H. (2020). Preparation, characterization and antioxidant activities of kelp phlorotannin nanoparticles. *Molecules, 25*(19), 4550. https://doi.org/10.3390/molecules25194550

Bhutto, R. A., Wang, M., Qi, Z., Hira, N. U. A., Jiang, J., Zhang, H., Iqbal, S., Wang, J., Stuart, M. A. C., & Guo, X. (2021). Pickering emulsions based on the pH-responsive assembly of food-grade chitosan. *ACS Omega, 6*(28), 17915–17922. https://doi.org/10.1021/acsomega.1c01490

Cai, X., Wang, Y., Du, X., Xing, X., & Zhu, G. (2020). Stability of pH-responsive Pickering emulsion stabilized by carboxymethyl starch/xanthan gum combinations. *Food Hydrocolloids, 109*(130), Article 106093. https://doi.org/10.1016/j.foodhyd.2020.106093

Chang, S. H., Lin, H. T. V., Wu, G. J., & Tsai, G. J. (2015). pH effects on solubility, zeta potential, and correlation between antibacterial activity and molecular weight of chitosan. *Carbohydr. Polym., 134*, 74–81. https://doi.org/10.1016/j.carbpol.2015.07.072

Chen, J., Mu, T., Zhang, M., & Goffin, D. (2018). Effect of heat treatments on the structure and emulsifying properties of protein isolates from cumin seeds (Cuminum cyminum). *Food Sci. Technol. Int., 24*(8), 673–687. https://doi.org/10.1177/1082013218788753

Chen, J., Mu, T., Zhang, M., & Goffin, D. (2019). Effect of high hydrostatic pressure on the structure, physicochemical and functional properties of protein isolates from cumin (Cuminum cyminum) seeds. *Int. J. Food Sci. Technol., 54*(3), 752–761. https://doi.org/10.1111/ijfs.13990

Chevalier, Y., & Bolzinger, M. A. (2013). Emulsions stabilized with solid nanoparticles: Pickering emulsions. *Collo. Surf. A. Physicochem. Eng. Asp., 439*, 23–34. https://doi.org/10.1016/j.colsurfa.2013.02.054

Daoud, S., Bou-maroun, E., Dujourdy, L., Waschatko, G., Billecke, N., & Cayot, P. (2019). Fast and direct analysis of oxidation levels of oil-in-water emulsions using ATR-FTIR. *Food Chemistry, 293*(December 2018), 307–314. https://doi.org/10.1016/j.foodchem.2019.05.005

Di Mattia, C. D., Sacchetti, G., Mastrocola, D., Sarker, D. K., & Pittia, P. (2010). Surface properties of phenolic compounds and their influence on the dispersion degree and oxidative stability of olive oil O/W emulsions. *Food Hydrocoll., 24*(6–7), 652–658. https://doi.org/10.1016/j.foodhyd.2010.03.007

Dong, X., Bai, Y., Xu, Z., Shi, Y., Sun, Y., Janaswamy, S., Yu, C., & Qi, H. (2019). Phlorotannins from undaria pinnatifida sporophyll: Extraction, antioxidant, and anti-inflammatory activities. *Marine Drugs, 17*(8), 434. https://doi.org/10.3390/md17080434

Flores-Molina, M. R., Rautenberger, R., Muñoz, P., Huovinen, P., & Gómez, I. (2016). Stress tolerance of the endemic Antarctic Brown alga Desmarestia anceps to UV radiation and temperature is mediated by high concentrations of phlorotannins. *Photochem. Photobiol., 92*(3), 455–466. https://doi.org/10.1111/php.12580

Ge, S., Jia, R., Li, Q., Liu, W., Liu, M., Cai, D., Zheng, M., Liu, H., & Liu, J. (2022). Pickering emulsion stabilized by zein/Adzuki bean seed coat polyphenol nanoparticles to enhance the stability and bioaccessibility of astaxanthin. *J. Funct. Foods, 88*, Article 104867. https://doi.org/10.1016/j.jff.2021.104867

Heffernan, N., Brunton, N. P., FitzGerald, R. J., & Smyth, T. J. (2015). Profiling of the molecular weight and structural isomer abundance of macroalgae-derived

phlorotannins. *Marine Drugs, 13*(1), 509–528. https://doi.org/10.3390/md13010509

Hu, J., Huang, C., Gong, A., Chen, H., Liu, S., Li, B., & Li, Y. (2020). Influence of pH on property and lipolysis behavior of cinnamaldehyde conjugated chitosan-stabilized emulsions. *Int. J. Biol. Macrom., 161*, 587–595. https://doi.org/10.1016/j.ijbiomac.2020.06.073

İlyasoğlu, H., Nadzieja, M., & Guo, Z. (2019). Caffeic acid grafted chitosan as a novel dual-functional stabilizer for food-grade emulsions and additive antioxidant property. *Food Hydrocolloids, 95*(April), 168–176. https://doi.org/10.1016/j.foodhyd.2019.04.043

Jo, M., Ban, C., Goh, K. K. T., & Choi, Y. J. (2021). Enhancement of the gut-retention time of resveratrol using waxy maize starch nanocrystal-stabilized and chitosan-coated Pickering emulsions. *Food Hydrocolloids, 112*(August 2020), Article 106291. https://doi.org/10.1016/j.foodhyd.2020.106291

Kasiri, N., & Fathi, M. (2018). Production of cellulose nanocrystals from pistachio shells and their application for stabilizing Pickering emulsions. *Int. J. Biol. Macrom., 106*, 1023–1031. https://doi.org/10.1016/j.ijbiomac.2017.08.112

Khan, N. M., Mu, T. H., Zhang, M., & Arogundade, L. A. (2014). The effects of pH and high hydrostatic pressure on the physicochemical properties of a sweet potato protein emulsion. *Food Hydrocoll., 35*, 209–216. https://doi.org/10.1016/j.foodhyd.2013.05.011

Klinkesorn, U. (2013). The role of chitosan in emulsion formation and stabilization. *Food Rev. Intl., 29*(4), 371–393. https://doi.org/10.1080/87559129.2013.818013

Li, D., Zhao, Y., Wang, X., Tang, H., Wu, N., Wu, F., Yu, D., & Elfalleh, W. (2020). Effects of (+)-catechin on a rice bran protein oil-in-water emulsion: Droplet size, zeta-potential, emulsifying properties, and rheological behavior. *Food Hydrocolloids, 98* (March 2019), Article 105306. https://doi.org/10.1016/j.foodhyd.2019.105306

Li, F., Li, X., Huang, K., Luo, Y., & Mei, X. (2021). Preparation and characterization of Pickering emulsion stabilized by hordein-chitosan complex particles. *Journal of Food Engineering, 292*(April 2020), Article 110275. https://doi.org/10.1016/j.jfoodeng.2020.110275

Li, X., & Xia, W. (2011). Effects of concentration, degree of deacetylation and molecular weight on emulsifying properties of chitosan. *Int. J. Biol. Macromol., 48*(5), 768–772. https://doi.org/10.1016/j.ijbiomac.2011.02.016

Liu, E., Zhao, S., Li, X., Meng, X., & Liu, B. (2021). Preparation, characterization of PLGA/chitosan nanoparticles as a delivery system for controlled release of DHA. *Int. J. Biol. Macromol., 185*(June), 782–791. https://doi.org/10.1016/j.ijbiomac.2021.06.190

Lundin, M., Macakova, L., Dedinaite, A., & Claesson, P. (2008). Interactions between chitosan and SDS at a low-charged silica substrate compared to interactions in the bulk - the effect of ionic strength. *Langmuir, 24*(8), 3814–3827. https://doi.org/10.1021/la702653m

Luo, D., Mu, T., & Sun, H. (2021). Profiling of phenolic acids and flavonoids in sweet potato (Ipomoea batatas L.) leaves and evaluation of their anti-oxidant and hypoglycemic activities. Food. *Bioscience, 39*, Article 100801. https://doi.org/10.1016/j.fbio.2020.100801

Lv, P., Wang, D., Chen, Y., Zhu, S., Zhang, J., Mao, L., Gao, Y., & Yuan, F. (2020). Pickering emulsion gels stabilized by novel complex particles of high-pressure-induced WPI gel and chitosan: Fabrication, characterization and encapsulation. *Food Hydrocoll., 108*(April), Article 105992. https://doi.org/10.1016/j.foodhyd.2020.105992

McClements, D. J., & Jafari, S. M. (2018). Improving emulsion formation, stability and performance using mixed emulsifiers: A review. *Adv. Colloid Interf. Sci., 251*, 55–79. https://doi.org/10.1016/j.cis.2017.12.001

Meng, W., Mu, T., Sun, H., & Garcia-Vaquero, M. (2021). Phlorotannins: A review of extraction methods, structural characteristics, bioactivities, bioavailability, and future trends. *Algal Research, 60*, Article 102484. https://doi.org/10.1016/j.algal.2021.102484

Meng, W., Mu, T., Sun, H., & Garcia-Vaquero, M. (2022). Evaluation of the chemical composition and nutritional potential of brown macroalgae commercialised in China. *Algal Research, 64*(March), Article 102683. https://doi.org/10.1016/j.algal.2022.102683

Meng, X., Liu, H., Dong, X., Wang, Q., Xia, Y., & Hu, X. (2022). A soft Pickering emulsifier made from chitosan and peptides endows stimuli-responsiveness, bioactivity and biocompatibility to emulsion. *Carbohydrate Polymers, 277*(October 2021), Article 118768. https://doi.org/10.1016/j.carbpol.2021.118768

Ming, Y., Xia, Y., & Ma, G. (2022). Aggregating particles on the O/W interface: Tuning Pickering emulsion for the enhanced drug delivery systems. *Aggregate*, 1–19, 10.1002/agt2.162.

Mudugamuwa Arachchige, M. P., Mu, T., & Ma, M. (2021). Effect of high hydrostatic pressure-assisted pectinase modification on the Pb2+ adsorption capacity of pectin isolated from sweet potato residue. *Chemosphere, 262*, Article 128102. https://doi.org/10.1016/j.chemosphere.2020.128102

Mwangi, W. W., Ho, K. W., Tey, B. T., & Chan, E. S. (2016). Effects of environmental factors on the physical stability of Pickering-emulsions stabilized by chitosan particles. *Food Hydrocoll., 60*, 543–550. https://doi.org/10.1016/j.foodhyd.2016.04.023

Noshad, M., Mohebbi, M., Koocheki, A., & Shahidi, F. (2016). Influence of interfacial engineering on stability of emulsions stabilized with soy protein isolate. *J.Dispers. Sci. Technol., 37*(1), 56–65. https://doi.org/10.1080/01932691.2015.1027907

Noshad, M., Mohebbi, M., Shahidi, F., & Koocheki, A. (2015). Effect of layer-by-layer polyelectrolyte method on encapsulation of vanillin. *Int. J. Biol. Macromol., 81*, 803–808. https://doi.org/10.1016/j.ijbiomac.2015.09.012

Shah, B. R., Dvořák, P., Velíšek, J., & Mráz, J. (2021). Opening a new gateway towards the applications of chitosan nanoparticles stabilized Pickering emulsion in the realm of aquaculture. *Carbohydr. Polym., 265*, Article 118096. https://doi.org/10.1016/j.carbpol.2021.118096

Shah, B. R., Xu, W., & Mráz, J. (2021). Fabrication, stability and rheological properties of zein/chitosan particles stabilized Pickering emulsions with antioxidant activities of the encapsulated vit-D3. *Int. J. Biol. Macromol., 191*(September), 803–810. https://doi.org/10.1016/j.ijbiomac.2021.09.159

Sharkawy, A., Barreiro, M. F., & Rodrigues, A. E. (2020). Chitosan-based Pickering emulsions and their applications: A review. *Carbohydrate Polymers, 250*(August), Article 116885. https://doi.org/10.1016/j.carbpol.2020.116885

Sionkowska, A., Kaczmarek, B., Gnatowska, M., & Kowalonek, J. (2015). The influence of UV-irradiation on chitosan modified by the tannic acid addition. *J. Photochem. Photobiol. B Biol., 148*, 333–339. https://doi.org/10.1016/j.jphotobiol.2015.03.028

Staroszczyk, H., Sztuka, K., Wolska, J., & Kołodziejska, I. (2014). In *, 117. Interactions of fish gelatin and chitosan in uncrosslinked and crosslinked with EDC films: FT-IR study. Spectrochimica Acta - Part A: Molecular and Biomolecular Spectroscopy* (pp. 707–712), 10.1016/j.saa.2013.09.044.

Sultan, M., Elsayed, H., Abdelhakim, A. E. F., & Taha, G. (2022). Active packaging gelatin films based on chitosan/Arabic gum/coconut oil Pickering nano emulsions. *J. Appl. Pol. Sci., 139*(1), 1–18. https://doi.org/10.1002/app.51442

Tabatabaei, M., Ebrahimi, B., & Rajaei, A. (2022). Producing submicron chitosan-stabilized oil Pickering emulsion powder by an electrostatic collector-equipped spray dryer. *Carbohydrate Polymers, 294*(April), Article 119791. https://doi.org/10.1016/j.carbpol.2022.119791

Tabatabaei, M., Rajaei, A., Hosseini, E., Aghbashlo, M., Kumar, V., Su, S., & Lam, S. (2022). Effect of type of fatty acid attached to chitosan on walnut oil-in-water Pickering emulsion properties. *Carbohydrate Polymers, 291*(February), Article 119566. https://doi.org/10.1016/j.carbpol.2022.119566

Tong, X., Cao, J., Sun, M., Liao, P., Dai, S., Cui, W., Cheng, X., Li, Y., Jiang, L., & Wang, H. (2021). Physical and oxidative stability of oil-in-water (O/W) emulsions in the presence of protein (peptide): Characteristics analysis and bioinformatics prediction. *Lwt, 149*(May), Article 111782. https://doi.org/10.1016/j.lwt.2021.111782

Wang, L. J., Yin, S. W., Wu, L. Y., Qi, J. R., Guo, J., & Yang, X. Q. (2016). Fabrication and characterization of Pickering emulsions and oil gels stabilized by highly charged zein/chitosan complex particles (ZCCPs). *Food Chem., 213*, 462–469. https://doi.org/10.1016/j.foodchem.2016.06.119

Wang, S., Qu, D., Zhao, G., Yang, L., Zhu, L., Song, H., & Liu, H. (2022). Characterization of the structure and properties of the isolating interfacial layer of oil–water emulsions stabilized by soy hull polysaccharide: Effect of pH changes. *Food Chemistry, 370*(August 2021), Article 131029. https://doi.org/10.1016/j.foodchem.2021.131029

Xia, T., Xue, C., & Wei, Z. (2021). Physicochemical characteristics, applications and research trends of edible Pickering emulsions. *Trends in Food Science and Technology, 107*(August 2020), 1–15. https://doi.org/10.1016/j.tifs.2020.11.019

Xie, M., Hu, B., Wang, Y., & Zeng, X. (2014). Grafting of gallic acid onto chitosan enhances antioxidant activities and alters rheological properties of the copolymer. *J. Agric. Food Chem., 62*(37), 9128–9136. https://doi.org/10.1021/jf503207s

Yan, C., McClements, D. J., Zhu, Y., Zou, L., Zhou, W., & Liu, W. (2019). Fabrication of OSA Starch/Chitosan polysaccharide-based high internal phase emulsion via altering interfacial behaviors. *J.Agric. Food Chem., 67*(39), 10937–10946. https://doi.org/10.1021/acs.jafc.9b04009

Yi, J., Gan, C., Wen, Z., Fan, Y., & Wu, X. (2021). Development of pea protein and high methoxyl pectin colloidal particles stabilized high internal phase Pickering emulsions for β-carotene protection and delivery. *Food Hydrocoll., 113*(September 2020), Article 106497. https://doi.org/10.1016/j.foodhyd.2020.106497

Yoksan, R., Jirawutthiwongchai, J., & Arpo, K. (2010). Encapsulation of ascorbyl palmitate in chitosan nanoparticles by oil-in-water emulsion and ionic gelation processes. *Colloids Surf. B Biointerfaces, 76*(1), 292–297. https://doi.org/10.1016/j.colsurfb.2009.11.007

Zembyla, M., Murray, B. S., Radford, S. J., & Sarkar, A. (2019). Water-in-oil Pickering emulsions stabilized by an interfacial complex of water-insoluble polyphenol crystals and protein. *J. Coll.Interf. Sci., 548*, 88–99. https://doi.org/10.1016/j.jcis.2019.04.010

Zhang, F., Cai, X., Ding, L., & Wang, S. (2021). Effect of pH, ionic strength, chitosan deacetylation on the stability and rheological properties of O/W emulsions formulated with chitosan/casein complexes. *Food Hydrocoll., 111*(December 2019), Article 106211. https://doi.org/10.1016/j.foodhyd.2020.106211

Zhao, Q., Fan, L., Liu, Y., & Li, J. (2022). Recent advances on formation mechanism and functionality of chitosan-based conjugates and their application in o/w emulsion systems: A review. *Food Chem., 380*(November 2021), Article 131838. https://doi.org/10.1016/j.foodchem.2021.131838

Zhu, L., Mu, T., Ma, M., Sun, H., & Zhao, G. (2022). Nutritional composition, antioxidant activity, volatile compounds, and stability properties of sweet potato residues fermented with selected lactic acid bacteria and bifidobacteria. *Food Chem., 374*(July 2021), Article 131500. https://doi.org/10.1016/j.foodchem.2021.131500

Zhu, X., Chen, J., Hu, Y., Zhang, N., Fu, Y., & Chen, X. (2021). Tuning complexation of carboxymethyl cellulose/ cationic chitosan to stabilize Pickering emulsion for curcumin encapsulation. *Food Hydrocoll., 110*(June 2020), Article 106135. https://doi.org/10.1016/j.foodhyd.2020.106135

Zhu, X., Hou, X., Ma, B., Xu, H., & Yang, Y. (2019). Chitosan/gallnut tannins composite fiber with improved tensile, antibacterial and fluorescence properties. *Carbohydr. Polym., 226*(July), Article 115311. https://doi.org/10.1016/j.carbpol.2019.115311